

Cathepsin L is required for endothelial progenitor cell-induced neovascularization

Carmen Urbich, Christopher Heeschen, Alexandra Aicher¹, Ken-ichiro Sasaki¹, Thomas Bruhl¹, Mohammad R Farhadi², Peter Vajkoczy², Wolf K Hofmann³, Christoph Peters⁴, Len A Pennacchio⁵, Nasreddin D Abolmaali⁶, Emmanouil Chavakis¹, Thomas Reinheckel⁴, Andreas M Zeiher¹ & Stefanie Dimmeler¹

Infusion of endothelial progenitor cells (EPC), but not of mature endothelial cells, promotes neovascularization after ischemia. We performed gene expression profiling of EPC and endothelial cells to identify genes that might be important for the neovascularization capacity of EPC. Notably, the protease cathepsin L (CathL) was highly expressed in EPC as opposed to endothelial cells and was essential for matrix degradation and invasion by EPC *in vitro*. CathL-deficient mice showed impaired functional recovery following hind limb ischemia, supporting the concept of a crucial role for CathL in postnatal neovascularization. Infused CathL-deficient progenitor cells neither homed to sites of ischemia nor augmented neovascularization. Forced expression of CathL in mature endothelial cells considerably enhanced their invasive activity and sufficed to confer their capacity for neovascularization *in vivo*. We concluded that CathL has a critical role in the integration of circulating EPC into ischemic tissue and is required for EPC-mediated neovascularization.

Neovascularization is an important adaptation to rescue tissue from critical ischemia¹. Postnatal blood vessel formation was formerly thought to be attributed mainly to the migration and proliferation of preexisting, fully differentiated endothelial cells, a process referred to as angiogenesis^{2–4}. Recent studies provide increasing evidence that circulating bone marrow-derived EPC contribute substantially to adult blood vessel formation^{5,6}. Intravenous infusion of EPC after ischemia improves neovascularization and cardiac function not only in animal models^{7,8} but also in pilot clinical studies⁹. In contrast, infusion of mature endothelial cells did not affect neovascularization after hind limb ischemia or myocardial infarction^{7,10}. To gain insights into the molecular differences underlying the divergent neovascularization capacity of EPC versus mature endothelial cells, we performed a gene expression analysis. Our data indicate that EPC express high levels of cathepsins in comparison to endothelial cells.

Cathepsins comprise the catalytic classes of serine, aspartate and cysteine peptidases exhibiting endo- or exopeptidase activities. There is growing evidence for specific intra- and extracellular functions for these lysosomal enzymes, which have been shown to critically influence tumor invasion and metastasis^{11–13}. Here we show that high expression of cathepsins in EPC is a prerequisite for their invasive capacity and facilitates the homing of EPC to ischemic tissue.

RESULTS

Gene expression analysis of EPC versus HUVEC

Phenotypical characterization of peripheral blood-derived human EPC confirmed the expression of various endothelial marker proteins including VEGF receptor 2 (KDR), CD105, VE-cadherin, von Willebrand factor, CD146, CD31 and Nos3 (**Fig. 1a** and data not shown)^{9,14,15}. Transplantation of EPC into immunodeficient nude mice following hind limb ischemia significantly ($P < 0.01$) improved neovascularization (**Fig. 1b**), whereas infusion of human umbilical venous endothelial cells (HUVEC), CD14⁺ monocytic cells¹⁶ or CD3⁺ T lymphocytes did not improve neovascularization (**Fig. 1b** and **Supplementary Fig. 1** online). To explore the differences in gene expression among EPC, HUVEC and CD14⁺ monocytes, we performed a microarray analysis of about 9,000 genes (**Supplementary Methods** online). We identified 480 genes whose expression was increased (fivefold or greater) in EPC as compared to HUVEC. Among the most consistent classes expressed differentially, EPC strongly express a large series of lysosomal peptidases, including CathL, cathepsin D (CathD), cathepsin H and cathepsin O (**Fig. 1c** and **Supplementary Table 1** online).

CathD and CathL are important for tumor invasion and metastasis^{12,13}. Therefore, we confirmed the differing expression of these cathepsins at the protein level (**Fig. 2** and **Supplementary Methods** online). EPC showed significantly ($P < 0.05$) increased levels of CathL protein as compared to HUVEC, human microvascular endothelial cells, CD14⁺ monocytes,

¹Molecular Cardiology, Department of Internal Medicine III, University of Frankfurt, Theodor-Stern-Kai 7, 60590 Frankfurt, Germany. ²Department of Neurosurgery, Medical Faculty of the University of Heidelberg, Theodor-Kutzer-Ufer 1-3, 68167 Mannheim, Germany. ³Department of Hematology and Oncology, Internal Medicine I, University of Frankfurt, Theodor-Stern-Kai 7, 60590 Frankfurt, Germany. ⁴Department of Molecular Medicine and Cell Research, Albert-Ludwigs-University Freiburg, Stefan-Meier-Strasse 17, 79104 Freiburg, Germany. ⁵Department of Genome Sciences, Lawrence Berkeley National Laboratory, 1 Cyclotron Road, Berkeley, California 94720, USA. ⁶Institute for Diagnostic and Interventional Radiology, University of Frankfurt, Theodor-Stern-Kai 7, 60590 Frankfurt, Germany. Correspondence should be addressed to S.D. (dimmeler@em.uni-frankfurt.de).

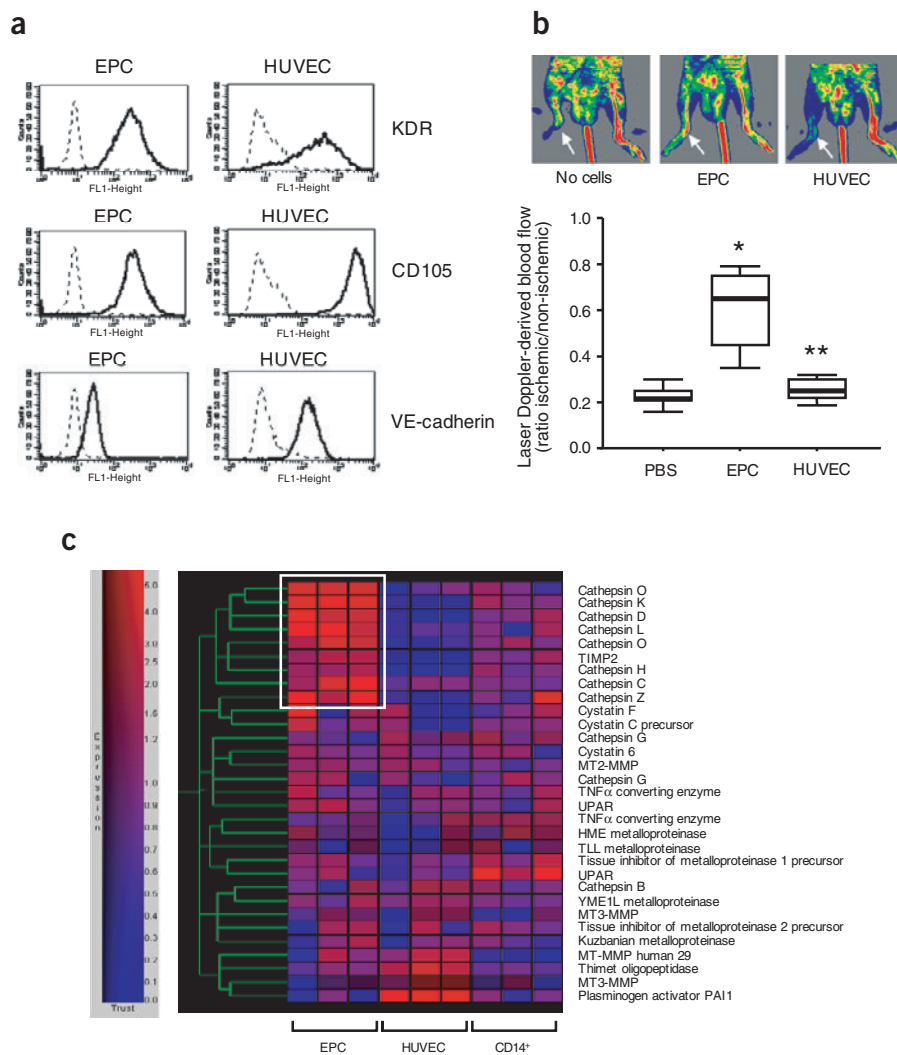


Figure 1 Gene expression analysis of EPC and HUVEC. **(a)** Expression of endothelial marker proteins in EPC (day 7 of culture) and HUVEC was measured by fluorescence-activated cell sorting analysis. Staining of KDR, CD105 and VE-cadherin (bold lines) is shown compared to isotype controls (dotted lines). Representative images of at least 3 independent experiments are shown. **(b)** PBS, HUVEC or EPC (8×10^5 cells each) were injected into nude mice ($n = 5$) after induction of hind limb ischemia. Results are shown as box plots representing median, 25th and 75th percentiles as boxes and the range of data as bars * $P = 0.001$ versus PBS, ** $P < 0.01$ versus EPC. Arrows indicate the ischemic leg. High perfusion is indicated by red, low perfusion by blue. **(c)** Total RNA of EPC, HUVEC and CD14⁺ monocytes (each $n = 3$) was isolated and the gene expression profile was assessed with the Affymetrix gene chip expression assay. A gene tree analysis is shown. The color scale is shown on the left. The brightness indicates the reliability. Blue indicates low expression, red indicates high expression.

Vasculogenesis, an important feature of ischemia-induced neovascularization¹, depends on various critical steps (Fig. 3b). Because cathepsins exert widespread substrate specificity, and thereby may influence different processes, we determined the potential involvement of CathL in each individual step. First, we assessed the mobilization of stem cells from the bone marrow in wild-type and *Ctsl*^{-/-} mice. But mobilization induced by hematopoietic growth factors (stem cell factor: 300 $\mu\text{g}/\text{kg}$ and granulocyte colony-stimulating factor: 250 $\mu\text{g}/\text{kg}$ daily for 3 d) was not impaired in *Ctsl*^{-/-} mice (wild-type showed a $258.8 \pm 37\%$ increase versus *Ctsl*^{-/-} $342.6 \pm 65\%$ increase in c-kit⁺ Sca-1⁺ cells in peripheral

blood). Moreover, adhesion of cultivated EPC to different matrices (Fig. 3c), to tumor necrosis factor- α -stimulated HUVEC (data not shown), or to denuded arteries *in vivo* was not modulated by pharmacological inhibition of CathL with Z-FF-FMK (Fig. 3d, Supplementary Fig. 3 and Supplementary Methods online). Inhibition of CathL in human EPC or genetic ablation using *Ctsl*^{-/-} cells also did not result in a significant change in proliferation, apoptosis or migration of EPC (Supplementary Fig. 3 and Supplementary Methods online). The release of growth-promoting factors from EPC also was similarly not affected by inhibition of CathL (data not shown). Finally, we showed that CathL does not modulate the angiogenic capacity of mature endothelial cells (Supplementary Fig. 4 and Supplementary Methods online). Thus, our data indicate that CathL is not critically involved in the regulation of EPC mobilization, survival, proliferation, migration or the angiogenic activity of mature endothelial cells.

Role of CathL in vasculogenesis and angiogenesis

Because CathL activity was specifically increased in EPC, we investigated the functional role of CathL in postnatal neovascularization using a hind limb ischemia model. Genetic ablation of CathL expression caused a significant ($P < 0.05$) impairment of neovascularization in CathL-deficient (*Ctsl*^{-/-}) mice (Fig. 3a), indicating that CathL is critical for ischemia-induced neovascularization.

Because cathepsins are matrix-degrading enzymes, we hypothesized that CathL contributes, instead, to the invasive capacity of EPC. EPC showed a more than twentyfold higher invasive capacity as compared to HUVEC and a significantly ($P < 0.05$) higher invasion than CD14⁺ monocytes (Fig. 4a). Incubation of EPC with the CathL inhibitor significantly ($P < 0.05$) reduced the cells' invasive capacity (Fig. 4a). In addition, incubation of EPC with cystatin C, a general inhibitor of papain-like cysteine peptidases (e.g., cathepsins B, H and L), also

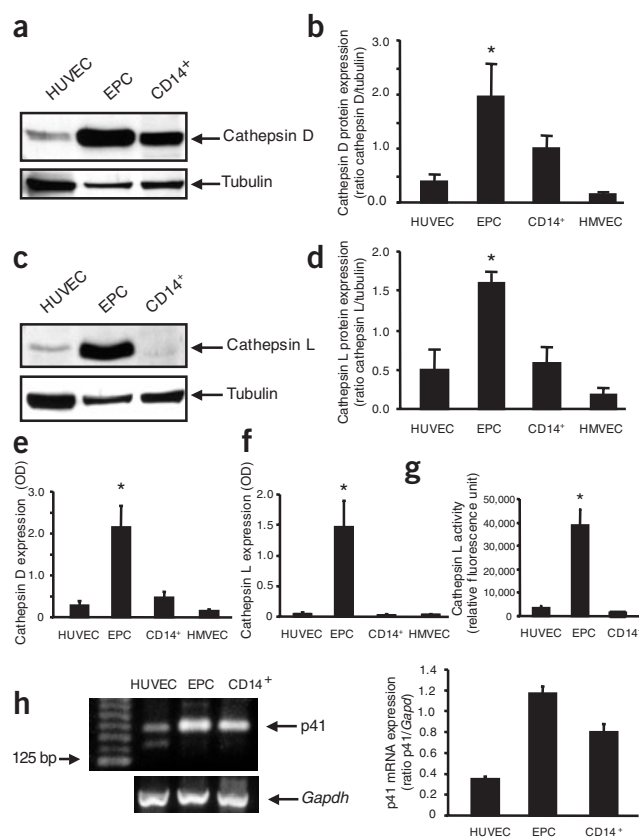
incubation of EPC with the CathL inhibitor significantly ($P < 0.05$) reduced the cells' invasive capacity (Fig. 4a). In addition, incubation of EPC with cystatin C, a general inhibitor of papain-like cysteine peptidases (e.g., cathepsins B, H and L), also

Figure 2 The expression and activity of cathepsin L is increased in EPC.

(a–d) HUVEC, EPC, CD14⁺ monocytes and human microvascular endothelial cells were lysed. The protein expression of CathD (a) or CathL (c) was analyzed by western blot. Tubulin serves as a loading control. A representative blot of four independent experiments is shown. (b,d) Blots were scanned and protein expression was quantified by densitometric analysis. The ratio of CathD/tubulin (b) or CathL/tubulin (d) is shown. $n = 3-5$; * $P < 0.05$ versus HUVEC. (e,f) HUVEC, EPC, CD14⁺ monocytes and human microvascular endothelial cells were lysed and the amount of CathD (e) or CathL (f) was measured by immunoassay. $n = 4$; * $P < 0.05$ versus HUVEC. (g) CathL activity was measured in HUVEC, EPC and CD14⁺ monocytes. $n \geq 3$; * $P < 0.05$ versus HUVEC. (h) The mRNA expression of p41 was measured by RT-PCR. A representative gel electrophoresis is shown (left panel). *Gapdh* serves as control. Quantification is shown in the right panel ($n = 3$).

significantly ($P < 0.05$) decreased EPC invasiveness, whereas the cathepsin S (CathS)-inhibitor (Z-Phe-Leu-COCHO)¹⁸, matrix metalloproteinase (MMP) inhibitors (GM6001 for MMP-3, GM1489 for MMP-9) and elastase inhibitors did not (Fig. 4a and data not shown). A cytotoxic effect of the inhibitors on EPC was excluded by measuring apoptosis and necrosis (data not shown). Moreover, we confirmed that the inhibitor of CathL did not affect MMP-2 and MMP-9 activity in EPC (data not shown).

To identify potential CathL targets involved in permitting EPC invasion, we determined the matrix degradation activity. Because CathL has been shown previously to degrade the matrix components gelatin and collagen¹⁹, we assessed the proteolytic activity of EPC extracts by zymography. EPC extracts showed high matrix-degrading activity, which was abolished by pharmacological inhibition of CathL (Fig. 4b,c). Moreover, active CathL as well as CathL inhibitor-sensitive gelatinolytic activities were detected in EPC culture supernatants (Fig. 4d,e, Supplementary Fig. 5 and Supplementary Methods online). Thus, active CathL is secreted by EPC, promoting extracellular degradation of matrix proteins. To determine whether the extracellular matrix proteolytic activity is linked to EPC invasion, we measured the degradation of the quenched fluorescent substrate DQ gelatin



in a three-dimensional Matrigel assay. Confocal images showed that invading EPC degraded matrix protein (Supplementary Fig. 6 online). Extracellular matrix degradation was reduced by the CathL inhibitor (Supplementary Fig. 6 online). Similar results were observed using DQ collagen type IV as a substrate (data not shown). The

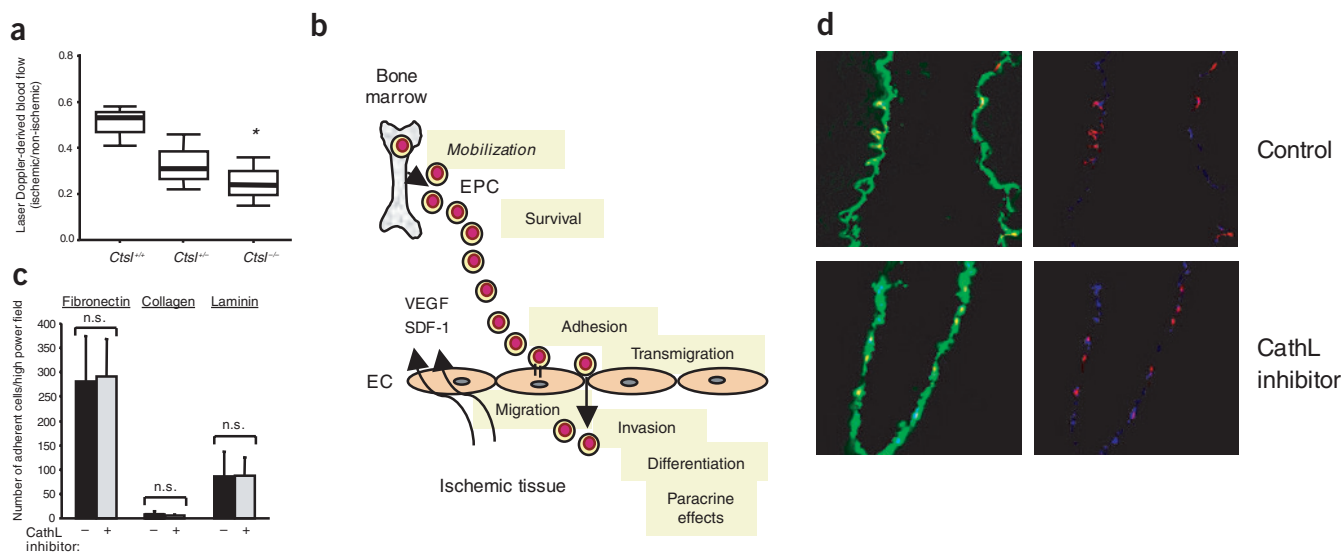


Figure 3 Role of CathL in neovascularization. (a) *Ctsl*^{+/+}, *Ctsl*^{+/-} or *Ctsl*^{-/-} mice were subjected to a model of hind limb ischemia. After 2 weeks, the ratio of blood flow in the ischemic (right) to normal (left) limb was measured with a laser Doppler blood flow meter. Results are shown as box plots representing median, 25th and 75th percentiles as boxes and the range of data as bars. $n = 3$, * $P < 0.05$ versus wild-type. (b) Schematic illustration of the multistep process of vasculogenesis. (c) EPC adhesion to different matrices ($n = 5$). (d) Re-endothelialization by EPC after balloon injury. Attachment and homing of CM-Dil-labeled EPC (red) to previously denuded arterial segments was assessed by staining cryosections for the endothelial marker von Willebrand factor (green) and the nuclear marker SYTOX (blue). Magnification, $\times 10$. n.s., not significant.

specific requirement of CathL for proteolysis of matrix proteins and invasion was further confirmed by using *Ctsl*^{-/-} progenitor cells (Fig. 4f,g). Proteolysis of fluorescence-labeled collagen and gelatin as well as gelatinolytic activity of cell lysates or supernatants were virtually absent in *Ctsl*^{-/-} cells (Fig. 4f and Supplementary Fig. 5 online). Moreover, the invasive activity of *Ctsl*^{-/-} Sca-1⁺ progenitor cells was significantly ($P < 0.05$) reduced as compared to wild-type cells (Fig. 4g). These data suggest that CathL is required for the extracellular matrix proteolysis and, subsequently, for the invasive capacity of progenitor cells in culture.

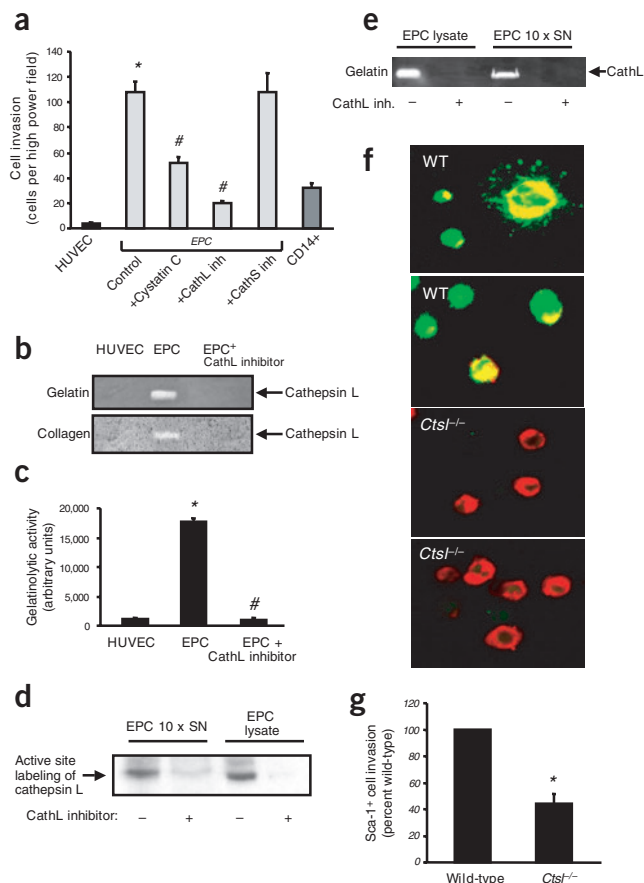


Figure 4 Role of CathL in EPC invasion. **(a)** The invasion of EPC, HUVEC and CD14⁺ monocytes was determined by two independent investigators (cells per high-power field). $n = 4$, * $P < 0.05$ versus HUVEC, # $P < 0.05$ versus EPC. **(b)** Cell lysates of HUVEC or EPC that were either untreated or pretreated with Z-FF-FMK (10 μ M; 2h) were analyzed by modified gelatin or collagen zymography. Representative zymographies are shown. **(c)** Densitometric quantification of the gelatin zymographies is shown. $n = 4$, * $P < 0.05$ versus HUVEC, # $P < 0.05$ versus EPC. **(d)** Cell lysates and ten-times concentrated cell culture supernatants (10 \times , SN) of EPC were incubated with biotin-labeled DCG-04 (10 μ M), which binds to active cysteine proteases. Lysates and supernatants were analyzed by western blot. A representative blot is shown. **(e)** CathL activity was analyzed in lysates and supernatants of EPC by modified gelatin zymography. A representative zymography is shown. **(f)** *In vivo* proteolysis of DQ gelatin was detected in CM-Dil-labeled wild-type or *Ctsl*^{-/-} bone marrow-derived Lin⁻ progenitor cells (red fluorescence). After incubation for 12 h at 37 $^{\circ}$ C, the proteolytic activity (green fluorescence) was determined by confocal microscopy. **(g)** The invasion of Sca-1⁺ bone marrow-derived cells of wild-type or *Ctsl*^{-/-} mice was measured using a modified Boyden chamber filled with Matrigel. Data are percent of wild-type, $n = 3$, * $P < 0.05$. Magnification, $\times 40$.

CathL contributes to EPC-mediated neovascularization *in vivo*

Having shown that CathL specifically affects EPC invasion, we investigated the effect of CathL on vascular integration and function of EPC during neovascularization *in vivo*. EPC were pretreated *ex vivo* with Z-FF-FMK or vehicle for 2 h prior to infusion. EPC were intravenously injected 24 h after unilateral induction of hind limb ischemia in nude mice. Mice receiving EPC pretreated with Z-FF-FMK showed significantly ($P < 0.01$) less improvement in limb perfusion as compared to mice receiving vehicle-treated EPC (Fig. 5a,b). Consistently, capillary density increased to a greater extent in mice receiving untreated EPC as compared to Z-FF-FMK-treated EPC (Fig. 5c and Supplementary Fig. 7 online). In addition, the number of small conductance vessels (<50 μ m) was significantly ($P < 0.05$) increased in mice receiving untreated EPC, whereas Z-FF-FMK-pretreated EPC abrogated this increase (Supplementary Fig. 8 online). Similar findings were obtained with mouse bone marrow-derived Lin⁻ Sca-1⁺ progenitor cells: Z-FF-FMK pretreatment abolished the Lin⁻ Sca-1⁺ progenitor cell-mediated improvement in neovascularization (Supplementary Fig. 9 online). Early EPC homing to the site of ischemia was investigated *in vivo* by magnetic resonance imaging (MRI) after labeling of EPC with iron particles. In the 'turbo inversion recovery magnitude' images, the area of ischemia is visualized by a strong hyperintensity as compared to the contralateral limb (Fig. 5d). In the T2* images, which were used for the assessment of tissue iron content, homing of untreated EPC after 24 h led to a marked signal extinction (iron artifact), whereas in animals receiving EPC pretreated with Z-FF-FMK, we observed no loss in signal intensity, suggesting a considerable reduction in early EPC homing (Fig. 5d).

Histological analysis of muscle sections harvested on day 14 consistently showed that the incorporation of human EPC into vascular structures was significantly ($P < 0.05$) reduced in mice receiving EPC pretreated with Z-FF-FMK. Incorporated cells were identified by double staining for human leukocyte antigen or labeling with CM-Dil to detect transplanted human EPC, in combination with the endothelial markers CD146, von Willebrand factor or CD31 (Fig. 5e,f, Supplementary Methods and Supplementary Fig. 10 online).

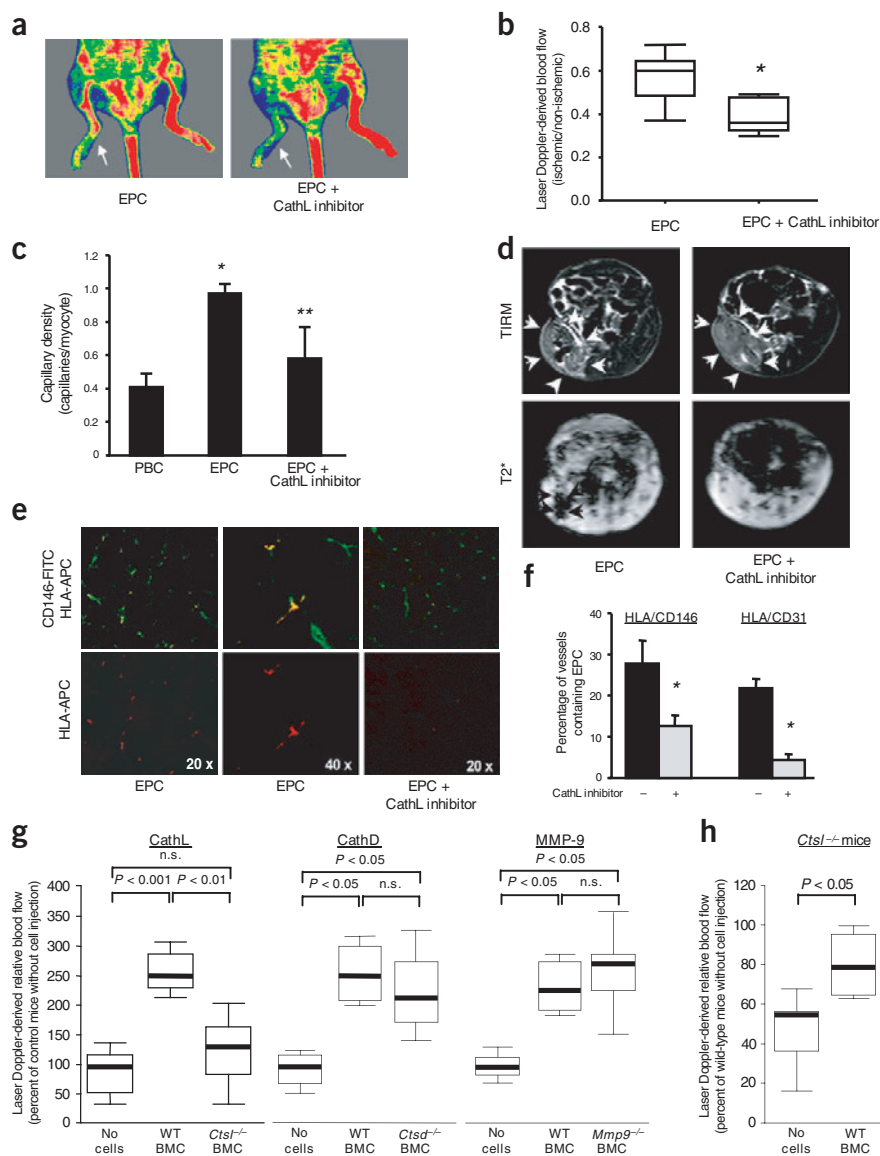
We used intravital fluorescence videomicroscopy to monitor the effects of pretreatment with the CathL inhibitor on homing and incorporation of progenitor cells into tumor vessels (Supplementary Methods online). Within 3 d after infusion, untreated progenitor cells adhered to the endothelium of tumor blood vessels, extravasated into the tumor stroma, began to organize into cord-like structures and incorporated into the tumor microvasculature. In contrast, markedly fewer Z-FF-FMK-pretreated cells successfully extravasated into the tumor tissue and remained in an inactive state, as suggested by their persistent round morphology, lack of tumor stroma invasion and lack of incorporation into the tumor blood vessels (Supplementary Fig. 11 online). Control experiments confirmed that the viability of the Z-FF-FMK-treated cells was not affected (data not shown) and that CathL activity was completely inhibited for at least 48 h following Z-FF-FMK treatment (Supplementary Fig. 3 online).

We confirmed that CathL is required for the neovascularization capacity of progenitor cells using a gene-based approach. The improvement of neovascularization following hind limb ischemia was significantly ($P < 0.01$) reduced in mice receiving *Ctsl*^{-/-} bone marrow-derived cells as compared to mice treated with wild-type cells (Fig. 5g). Consistently, the increase in capillary density was significantly ($P = 0.023$) lower in mice treated with *Ctsl*^{-/-} bone marrow-derived cells ($133 \pm 16\%$) as compared to mice treated with wild-type cells ($261 \pm 46\%$). We determined the number of incorporated Y chromosome-positive cells derived from the male CathL-deficient donor mice by fluorescence *in situ* hybridization

Figure 5 CathL is required for improvement of neovascularization. Human EPC pretreated with or without the CathL inhibitor Z-FF-FMK (8×10^5 cells; each $n = 7-8$) were injected into nude mice after induction of ischemia. (a) Representative Doppler images 2 weeks after induction of hind limb ischemia are shown. Arrows indicate ischemic leg. (b) Results are shown as box plots representing median, 25th and 75th percentiles as boxes and the range of data as bars. * $P < 0.01$. (c) Capillary density was assessed by immunohistochemistry for CD31. $n = 4$, * $P < 0.05$ versus phosphate-buffered saline, ** $P < 0.05$ versus EPC. (d) Early homing of iron-labeled EPC to the area of ischemia assessed by MRI. Area of ischemia indicated by white arrows; iron content indicated by black arrows. (e, f) Long-term incorporation of EPC was assessed by immunohistochemistry for CD146-FITC or CD31-FITC (green) and HLA-A,B,C-APC (red). * $P < 0.05$ versus untreated EPC, $n = 4$. (g) Wild-type, *Ctsl*^{-/-}, *Ctsd*^{-/-} or *Mmp9*^{-/-} bone marrow mononuclear cells (10^6 cells; each $n \geq 4$ BMC-treated animals per group) were injected into nude mice after induction of ischemia. Laser Doppler images were quantified. Box plots representing median, 25th and 75th percentiles as boxes and the range of data as bars are shown. (h) *Ctsl*^{-/-} mice were subjected to hind limb ischemia. Wild-type BMC were injected (2×10^6 cells) into *Ctsl*^{-/-} mice 24 h after induction of ischemia. After 2 weeks limb blood flow ratio was measured with a laser Doppler blood flow meter. Results are shown as box plots representing median, 25th and 75th percentiles as boxes and the range of data as bars, $n \geq 4$.

(FISH; **Supplementary Fig. 12** online). The vascular incorporation of *Ctsl*^{-/-} cells was significantly ($P < 0.05$) reduced to $45.5 \pm 9.2\%$ relative to wild-type cells. To ascertain if the effect of CathL was specific, by comparison to other proteases, we next infused cells from MMP-9- or CathD-deficient (*Ctsd*^{-/-} mice using the same nude mouse model of hind limb ischemia. Neither *Ctsd*^{-/-} nor *Mmp9*^{-/-} bone marrow-derived cells showed reduced neovascularization capacity as compared to wild-type cells (**Fig. 5g**). These data suggest that the lack of CathL specifically impairs the functional incorporation of bone marrow-derived progenitor cells, which may account for the impaired neovascularization capacity of *Ctsl*^{-/-} mice. Indeed, the reduced neovascularization of *Ctsl*^{-/-} mice was at least partially reversed by infusion of wild-type cells (**Fig. 5h**).

Finally, we determined the contribution of bone marrow-derived circulating progenitor cells to the increased protease activity found in ischemic tissues *in vivo*. For this purpose, mice were lethally irradiated to ablate the bone marrow before the induction of hind limb ischemia. Forty-eight hours after induction of ischemia, muscle lysates of the ischemic and nonischemic limbs were analyzed by zymography and western blot. As shown in **Supplementary Fig. 13** online, CathL and MMP-9 activities were significantly ($P < 0.05$) induced in ischemic tissue. In irradiated mice, MMP-9 activity was still significantly ($P < 0.05$) upregulated after ischemia (**Supplementary Fig. 13** online), indicating that MMP-9 activity is increased independent of bone marrow-derived cells and hence is likely generated by cells that reside in the tissue. In contrast, ischemia-induced augmentation of CathL activity was abolished



in irradiated mice (**Supplementary Fig. 13** online), showing that the increase of CathL activity in ischemic tissue is mediated by irradiation-sensitive cells that probably originate from the bone marrow.

CathL improves neovascularization capacity of HUVEC

To investigate whether ectopic expression of CathL in mature endothelial cells might suffice to generate cells that are capable of promoting neovascularization after intravenous infusion, HUVEC were transiently transfected with CathL prior to injection into nude mice after induction of ischemia. The infusion of CathL-transfected HUVEC significantly ($P < 0.05$) increased the recovery of limb perfusion as compared to vector-transfected cells (**Fig. 6a**). Control experiments confirmed that transfection of HUVEC with CathL resulted in an increased CathL expression and activity (**Fig. 6b,c**) and subsequently enhanced their invasive capacity *in vitro* (**Fig. 6d**). Likewise, infusion of isolated mature aortic endothelial cells from transgenic mice expressing CathL also improved neovascularization following hind limb ischemia ($135 \pm 16\%$ of control; $n = 3$). In contrast, transient expression of a nonsecretable CathL mutant²⁰ did not improve neovascularization of HUVEC (**Fig. 6a**).

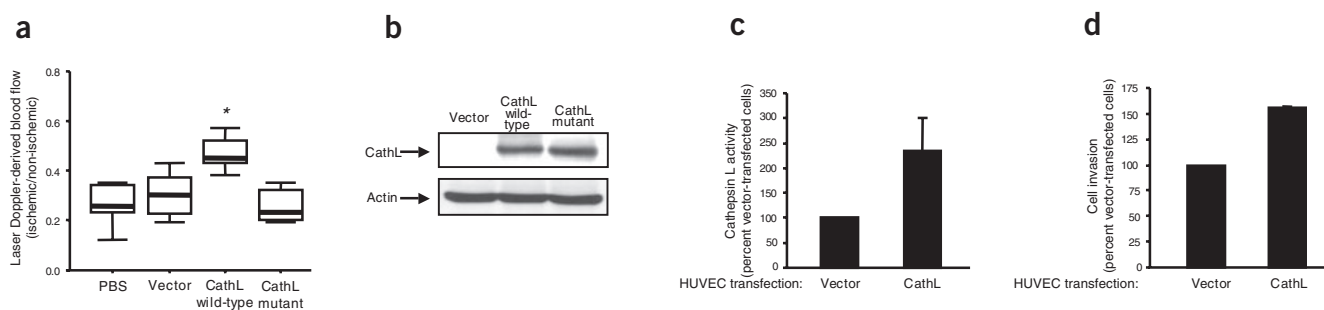


Figure 6 Overexpression of CathL in mature endothelial cells partially rescued the impaired improvement of neovascularization. HUVEC were transfected for 24 h. **(a)** The cells (1.5×10^6 cells; each $n \geq 4$) were injected into nude mice after induction of hind limb ischemia. Laser Doppler-derived relative blood flow was measured 2 weeks after induction of ischemia. Results are shown as box plots representing median, 25th and 75th percentiles as boxes and the range of data as bars * $P < 0.05$ versus vector-transfected cells and versus CathL mutant-transfected cells. **(b)** CathL wild-type or mutant was detected by western blot analysis. Actin serves as a loading control. A representative blot is shown. **(c)** CathL activity. Data are percent of vector-transfected cells, $n = 3$. **(d)** *In vitro* invasion was determined in a modified Boyden chamber filled with Matrigel. Data are percent of vector-transfected cells, $n = 3$.

DISCUSSION

Proteases are of major importance for the formation of new blood vessels^{21–23}. In order to form sprouts, endothelial cells must penetrate the extracellular matrix, which consists of type IV collagen, laminin, fibronectin and many other macromolecules. For this purpose, mature endothelial cells are equipped with a set of proteases including MMPs and the urokinase-type plasminogen activator. Notably, our study indicates that circulating progenitor cells express a distinct pattern of proteases. *Ex vivo* cultivated peripheral blood-derived EPC showed profoundly increased levels of cathepsins as compared to mature endothelial cells, monocytes and lymphocytes. These broad-spectrum proteases are potent in degrading several extracellular matrix proteins such as laminin, fibronectin, collagens I and IV, elastin and other structural proteins of basement membranes (reviewed in refs. 24,25). Notably, EPC secrete large amounts of CathL and the extracellular matrix-degrading activity of EPC toward gelatin or collagen is abolished by pharmacological inhibition or genetic ablation of CathL.

Given the overlapping substrate specificity of lysosomal proteases, it is notable that CathL seems to be of particular importance for EPC invasion. Previous studies using CathL knockout animals provide evidence for biological effects being specifically mediated by CathL^{26,27}. In line with these findings, our results show that the recovery from hind limb ischemia is substantially impaired in *Ctsl*^{-/-} mice. Moreover, pharmacological inhibition of CathL abolished the matrix-degrading activity of EPC extracts or cell culture supernatants. CathS was recently shown to contribute to angiogenesis²⁸. In our experiments, however, pharmacological inhibition of CathS did not affect EPC invasion. Moreover, genetic ablation of another related member of the cathepsin family, CathD, did not reduce the ability of bone marrow-derived stem cells to promote neovascularization following ischemia. Moreover, pharmacological inhibition of other proteases such as elastases or MMPs did not affect the invasive activity of EPC *in vitro*. In line with these *in vitro* findings, MMP-9-deficient progenitor cells showed no impaired ability to augment neovascularization *in vivo*. Likewise, the increase of MMP-9 activity after induction of ischemia was independent of bone marrow-derived cells, but rather reflects an increased local release by cells that reside in the tissues. In contrast, the observed upregulation of CathL following ischemia was abolished by irradiation-induced bone marrow ablation. Thus, our data indicate that CathL has a specific and crucial role, as opposed to other cathepsins or MMP-9, for EPC function in neovascularization.

The impairment of neovascularization in *Ctsl*^{-/-} mice may be related to a reduction in functional activity of mature endothelial cells from *Ctsl*^{-/-} mice resulting in impaired angiogenesis or a reduced capacity of EPC to promote vasculogenesis. Because we showed that pharmacological CathL inhibitors and genetic depletion of CathL did not affect the proangiogenic activity of mature endothelial cells, interference with the classical angiogenesis pathway by blocking or deleting CathL seems unlikely. In contrast, CathL may contribute to vasculogenesis specifically by promoting the invasive activity of EPC, as opposed to EPC mobilization, adhesion, survival or migration. Inhibition or genetic ablation of CathL specifically reduced the invasive potential of EPC *in vitro*. Moreover, inhibition of CathL blocked the invasion and incorporation of EPC into tumor capillaries *in vivo* and reduced the incorporation and functional activity of EPC in the hind limb ischemia model. But the finding that most of our studies show only partial inhibition of neovascularization by pharmacological or genetic depletion of CathL indicates that other proteases or adhesion molecules support the incorporation of EPC into the ischemic limbs.

Taken together, the present findings show a critical role for CathL in the invasive and functional capacity of EPC. The high expression levels of CathL in EPC equip these cells for 'drilling for oxygen' to promote blood supply to ischemic tissues. In contrast, inhibition of the invasive potential of circulating progenitor cells by CathL inhibitors may be an attractive target for limiting tumor vascularization, which is critically dependent on EPC invasion^{29,30}.

METHODS

Generation of CathL-deficient mice and transgenic mice overexpressing human CathL. CathL-deficient mice were generated by gene targeting in mouse embryonic stem cells as described^{31,32}. Expression of *Ctsl* mRNA, CathL protein and activity was completely abolished in CathL-deficient mice³². CathL-transgenic mice were generated as previously described³³. CathD- and MMP-9-deficient mice have been generated as described^{34,35}.

Plasmid transfection. A plasmid encoding human full length pro-CathL was cloned by PCR from cDNA of EPC into pcDNA3.1-Myc-His (Invitrogen). We cloned a plasmid encoding the nonsecretable human pro-CathL delta TV mutant lacking the last two carboxy-terminal amino acids by PCR from full-length pro-CathL into pcDNA3.1-Myc-His as previously described²⁰. We performed transient transfection of HUVEC (24 h) as described previously³⁶.

***In vitro* invasion.** A modified Boyden chamber (Transwell, 8 μ m pore size, BD Falcon) was filled with Matrigel (4 mg/ml; BD Biosciences). We placed detached cells (10^5 cells) in the upper compartment of the cham-

ber in the presence or absence of cystatin C (10 nM), Z-FF-FMK (10 μ M) or Z-FL-COCHO (10 μ M, Calbiochem). After 24 h at 37 °C, we removed the chambers and manually counted the cells in the lower part of the culture plate.

Confocal proteolysis assay. *In vivo* proteolysis as previously described³⁷ was modified as follows: one half of a plastic ring was filled with 100 μ l Matrigel (10 mg/ml, BD Biosciences) containing the quenched fluorescent substrate DQ gelatin (25 μ g/ml, Molecular Probes) in the presence of VEGF (50 ng/ml) and SDF-1 (50 ng/ml). The other half of the ring was filled with 100 μ l Matrigel (10 mg/ml) containing 1×10^5 CM-Dil-labeled cells. After incubation for 12 h at 37 °C, the proteolytic activity (green fluorescence) was determined by confocal microscopy using a LSM 510.

Zymography. We concentrated cell culture supernatants (10 times) using Ultrafree-4 centrifugal filter tubes with Biomax-5 membrane (Millipore). We lysed cells in buffer (1% Triton-X-100, 1 mM EDTA, 1 mM EGTA, 150 mM NaCl, 1 mM PMSF, 20 mM Tris (pH 7.4), 2.5 mM Na-pyrophosphate, 1 mM β -glycerolphosphate, 1 mM Na-orthovanadate, 1 μ g/ml leupeptin). We analyzed metalloproteinase activity by gelatinolytic zymography as described³⁸. The gelatin and collagen zymography for acidic proteases was performed according to previous studies³⁹. After gel electrophoresis, the gels were washed twice for 20 min with 25% isopropanol to remove sodium dodecyl sulfate⁴⁰.

Mouse model of hind limb ischemia. This study was performed with permission of the State of Hesse, Regierungspraesidium Darmstadt, according to section 8 of the German Law for the Protection of Animals and conforms to the Guide for the Care and Use of Laboratory Animals measurements. The mouse model of hind limb ischemia was performed by use of 8–10-week-old athymic NMRI nude mice (Charles River) or as indicated. We ligated the proximal femoral artery including the superficial and the deep branch as well as the distal saphenous artery. We injected cells intravenously 24 h after induction of unilateral hind limb ischemia. Animals received untreated human EPC and pretreated EPC (Z-FF-FMK; 10 μ M; 2 h) or sex-mismatched bone marrow cells from male CathL-deficient and wild-type mice, respectively. We harvested bone marrow aseptically by flushing tibias and femurs of donor mice, filtered it (100 μ m) and isolated mononuclear cells by density gradient centrifugation. The use of human cells was approved by the Ethics Committee of the University of Frankfurt.

Limb perfusion. After 2 weeks, we measured the ratio of blood flow in the ischemic (right) to normal (left) limb with a laser Doppler blood flow meter (MoorLDI-Mark 2, Moor Instruments, Inc.). After recording laser Doppler color images, we calculated the average perfusions of the ischemic and non-ischemic limb on the basis of colored histogram pixels.

EPC tracking by magnetic resonance imaging (MRI). EPC were labeled with 0.9 μ m superparamagnetic divinyl benzene inert polymer microspheres (Bangs Laboratories)⁴¹ and intravenously injected 24 h after induction of ischemia. After another 24 h, we placed mice inside a small loop coil on a 1.5-Tesla system (Magnetom Sonata, Siemens). We performed two-dimensional MRI using turbo inversion recovery magnitude sequences to visualize the edema related to the ischemia and T2*-weighted gradient echo sequences to visualize the magnetic field distortion related to the presence of superparamagnetic particles-labeled EPC.

Histological evaluation. Capillary density was determined in 8- μ m frozen sections of the adductor and semimembraneous muscles. Endothelial cells were stained for CD146 (Chemicon) or CD31 (BD Biosciences), respectively. Capillary density is expressed as number of capillaries per myocyte. We identified human EPC by costaining for HLA-A, HLA-B and HLA-C (APC-labeled; BD Biosciences).

Statistical analysis. Results for continuous variables are expressed as mean \pm s.e.m. or as stated otherwise. Comparisons between groups were analyzed by t-test (two-sided) or ANOVA for experiments with more than two subgroups. Post hoc range tests and pairwise multiple comparisons were performed with t-test (two-sided) with Bonferroni adjustment. $P < 0.05$ was considered statistically significant. All analyses were performed with SPSS 11.5 software (SPSS Inc.).

Accession number. Microarray data from this study are available in the Gene Expression Omnibus using the accession number GSE2040.

Note: Supplementary information is available on the Nature Medicine website.

ACKNOWLEDGMENTS

We are thankful to J. Gille (University of Frankfurt, Frankfurt, Germany) and Z. Werb (University of California, San Francisco, California) for providing the MMP9-deficient mice. DCG-04 was donated by M. Bogyo (Stanford University Medical School, California). We would like to thank A. Knau, M. Näher, and M. Muhly-Reinholz for technical help. This study was supported by the Deutsche Forschungsgemeinschaft (Di 600/4-1, He 3044/2-2 and VA151/4-3), the Alfried Krupp Stiftung (S.D.), the Fonds der Chemischen Industrie (T.R. and C.P.), by the Deutsche Krebshilfe (T.R.), and in part by National Institutes of Health Grant HL071954A (DE-AC03-76SF00098 (L.A.P.)). K.S. was in part supported by the Japan Heart Foundation/Bayer Yakuhi Research Grant Abroad. The authors C.U., C.H., A.A., T.B., A.M.Z. and S.D. belong to the European Vascular Genomics Network (<http://www.evgn.org>) a Network of Excellence supported by the European Community's sixth Framework Programme for Research Priority 1 "Life sciences, genomics and biotechnology for health" (Contract number LSHM-CT-2003-503254).

COMPETING INTERESTS STATEMENT

The authors declare that they have no competing financial interests.

Received 17 October; accepted 16 December 2004

Published online at <http://www.nature.com/naturemedicine/>

- Isner, J.M. & Asahara, T. Angiogenesis and vasculogenesis as therapeutic strategies for postnatal neovascularization. *J. Clin. Invest.* **103**, 1231–1236 (1999).
- Folkman, J. Angiogenesis in cancer, vascular, rheumatoid and other disease. *Nat. Med.* **1**, 27–31 (1995).
- Risau, W. Mechanisms of angiogenesis. *Nature* **386**, 671–674 (1997).
- Carmeliet, P. & Jain, R.K. Angiogenesis in cancer and other diseases. *Nature* **407**, 249–257 (2000).
- Asahara, T. *et al.* Isolation of putative progenitor endothelial cells for angiogenesis. *Science* **275**, 964–967 (1997).
- Shi, Q. *et al.* Evidence for circulating bone marrow-derived endothelial cells. *Blood* **92**, 362–367 (1998).
- Kalka, C. *et al.* Transplantation of ex vivo expanded endothelial progenitor cells for therapeutic neovascularization. *Proc. Natl. Acad. Sci. USA* **97**, 3422–3427 (2000).
- Kawamoto, A. *et al.* Therapeutic potential of ex vivo expanded endothelial progenitor cells for myocardial ischemia. *Circulation* **103**, 634–647 (2001).
- Assmus, B. *et al.* Transplantation of Progenitor Cells and Regeneration Enhancement in Acute Myocardial Infarction (TOPCARE-AMI). *Circulation* **106**, 3009–3017 (2002).
- Kocher, A.A. *et al.* Neovascularization of ischemic myocardium by human bone-marrow-derived angioblasts prevents cardiomyocyte apoptosis, reduces remodeling and improves cardiac function. *Nat. Med.* **7**, 430–436 (2001).
- Joyce, J.A. *et al.* Cathepsin cysteine proteases are effectors of invasive growth and angiogenesis during multistage tumorigenesis. *Cancer Cell* **5**, 443–453 (2004).
- Berchem, G. *et al.* Cathepsin-D affects multiple tumor progression steps *in vivo*: proliferation, angiogenesis and apoptosis. *Oncogene* **21**, 5951–5955 (2002).
- Krueger, S., Kellner, U., Buehling, F. & Roessner, A. Cathepsin L antisense oligonucleotides in a human osteosarcoma cell line: effects on the invasive phenotype. *Cancer Gene Ther.* **8**, 522–528 (2001).
- Dimmeler, S. *et al.* HMG-CoA reductase inhibitors (statins) increase endothelial progenitor cells via the PI 3-kinase/Akt pathway. *J. Clin. Invest.* **108**, 391–397. (2001).
- Vasa, M. *et al.* Number and migratory activity of circulating endothelial progenitor cells inversely correlate with risk factors for coronary artery disease. *Circ. Res.* **89**, E1–7 (2001).
- Urbich, C. *et al.* Relevance of monocytic features for neovascularization capacity of circulating endothelial progenitor cells. *Circulation* **108**, 2511–2516 (2003).
- Fiebigler, E. *et al.* Invariant chain controls the activity of extracellular cathepsin L. *J. Exp. Med.* **196**, 1263–1269 (2002).
- Walker, B., Lynas, J.F., Meighan, M.A. & Bromme, D. Evaluation of dipeptide alpha-keto-beta-aldehydes as new inhibitors of cathepsin S. *Biochem. Biophys. Res. Commun.* **275**, 401–405 (2000).
- Li, Z. *et al.* Regulation of collagenase activities of human cathepsins by glycosaminoglycans. *J. Biol. Chem.* **279**, 5470–5479 (2004).
- Chauhan, S.S., Ray, D., Kane, S.E., Willingham, M.C. & Gottesman, M.M. Involvement of carboxy-terminal amino acids in secretion of human lysosomal protease cathepsin L. *Biochemistry* **37**, 8584–8594 (1998).
- Libby, P. & Schonbeck, U. Drilling for oxygen: angiogenesis involves proteolysis of the extracellular matrix. *Circ. Res.* **89**, 195–197 (2001).
- Carmeliet, P. Mechanisms of angiogenesis and arteriogenesis. *Nat. Med.* **6**, 389–395 (2000).
- Devy, L. *et al.* The pro- or antiangiogenic effect of plasminogen activator inhibitor 1 is dose dependent. *FASEB J.* **16**, 147–154 (2002).
- Rooprai, H.K. & McCormick, D. Proteases and their inhibitors in human brain tumours: a review. *Anticancer Res.* **17**, 4151–4162 (1997).
- Turk, V., Turk, B. & Turk, D. Lysosomal cysteine proteases: facts and opportunities.

- EMBO J.* **20**, 4629–4633 (2001).
26. Stypmann, J. *et al.* Dilated cardiomyopathy in mice deficient for the lysosomal cysteine peptidase cathepsin L. *Proc. Natl. Acad. Sci. USA* **99**, 6234–6239 (2002).
 27. Tobin, D.J. *et al.* The lysosomal protease cathepsin L is an important regulator of keratinocyte and melanocyte differentiation during hair follicle morphogenesis and cycling. *Am. J. Pathol.* **160**, 1807–1821 (2002).
 28. Shi, G.P. *et al.* Deficiency of the cysteine protease cathepsin S impairs microvessel growth. *Circ. Res.* **92**, 493–500 (2003).
 29. Lyden, D. *et al.* Impaired recruitment of bone-marrow-derived endothelial and hematopoietic precursor cells blocks tumor angiogenesis and growth. *Nat. Med.* **7**, 1194–1201 (2001).
 30. Rafii, S., Lyden, D., Benezra, R., Hattori, K. & Heissig, B. Vascular and haematopoietic stem cells: novel targets for anti-angiogenesis therapy? *Nat. Rev. Cancer* **2**, 826–835 (2002).
 31. Nakagawa, T. *et al.* Cathepsin L: critical role in li degradation and CD4 T cell selection in the thymus. *Science* **280**, 450–453 (1998).
 32. Roth, W. *et al.* Cathepsin L deficiency as molecular defect of furless: hyperproliferation of keratinocytes and perturbation of hair follicle cycling. *FASEB J.* **14**, 2075–2086 (2000).
 33. Houseweart, M.K. *et al.* Cathepsin B but not cathepsins L or S contributes to the pathogenesis of Unverricht-Lundborg progressive myoclonus epilepsy (EPM1). *J. Neurobiol.* **56**, 315–327 (2003).
 34. Saftig, P. *et al.* Mice deficient for the lysosomal proteinase cathepsin D exhibit progressive atrophy of the intestinal mucosa and profound destruction of lymphoid cells. *EMBO J.* **14**, 3599–3608 (1995).
 35. Lelongt, B. *et al.* Matrix metalloproteinase 9 protects mice from anti-glomerular basement membrane nephritis through its fibrinolytic activity. *J. Exp. Med.* **193**, 793–802 (2001).
 36. Urbich, C. *et al.* Dephosphorylation of endothelial nitric oxide synthase contributes to the anti-angiogenic effects of endostatin. *FASEB J.* **16**, 706–708 (2002).
 37. Premzl, A., Zavasnik-Bergant, V., Turk, V. & Kos, J. Intracellular and extracellular cathepsin B facilitate invasion of MCF-10A neoT cells through reconstituted extracellular matrix in vitro. *Exp. Cell. Res.* **283**, 206–214 (2003).
 38. Aicher, A. *et al.* Essential role of endothelial nitric oxide synthase for mobilization of stem and progenitor cells. *Nat. Med.* **9**, 1370–1376 (2003).
 39. Denhoffer, R. *et al.* Invasion of melanoma cells into dermal connective tissue in vitro: evidence for an important role of cysteine proteases. *Int. J. Cancer* **106**, 316–323 (2003).
 40. Kaberdin, V.R. & McDowall, K.J. Expanding the use of zymography by the chemical linkage of small, defined substrates to the gel matrix. *Genome Res.* **13**, 1961–1965 (2003).
 41. Hinds, K.A. *et al.* Highly efficient endosomal labeling of progenitor and stem cells with large magnetic particles allows magnetic resonance imaging of single cells. *Blood* **102**, 867–872 (2003).